

## Resonant Raman scattering probe of alloying effect in ZnMgO thin films

J. F. Kong,<sup>1</sup> W. Z. Shen,<sup>1,a)</sup> Y. W. Zhang,<sup>2</sup> C. Yang,<sup>2</sup> and X. M. Li<sup>2</sup>

<sup>1</sup>Laboratory of Condensed Matter Spectroscopy and Opto-Electronic Physics, Department of Physics, Shanghai Jiao Tong University, 1954 Hua Shan Road, Shanghai 200030, People's Republic of China

<sup>2</sup>State Key Laboratory of High Performance Ceramics and Superfine Microstructures, Shanghai Institute of Ceramics, Chinese Academy of Sciences, 1295 Ding Xi Road, Shanghai 200050, People's Republic of China

(Received 31 March 2008; accepted 28 April 2008; published online 15 May 2008)

We have presented a detailed resonant Raman scattering investigation for the alloying effect in hexagonal  $\text{Zn}_{1-x}\text{Mg}_x\text{O}$  ( $x \leq 0.323$ ) thin films grown by pulsed laser deposition. Alloy-induced longitudinal optical (LO) phonon resonance effect has been achieved from the Raman peak shift, lineshape, and intensity through changing the Mg composition and temperature to tune the ZnMgO bandgap. By the aid of theoretical analysis combining with the extrinsic Fröhlich interaction mediated via a localized exciton, we demonstrate the pronounced outgoing resonance behavior for the LO phonons in ZnMgO, where the localized exciton due to alloy disorder dominates the resonance processes. © 2008 American Institute of Physics. [DOI: 10.1063/1.2930676]

Resonant Raman scattering (RRS) has the advantage compared to other optical measurements, since it provides information about both the lattice dynamics and electronic structure of materials. This technique is especially important for alloy semiconductors, where the alloy-induced disorder perturbs the interaction between the lattice vibrations and electronic states, and introduces localized excitons in the forbidden gap shown as sharp resonance features in RRS.<sup>1</sup> A key issue in optimizing semiconductor diode lasers concerns the microscopic mechanism responsible for gain and stimulated emission, which can be appropriately examined by the strong localized excitonic effects.<sup>2</sup> Therefore, RRS has been demonstrated to be an important tool in studying the optoelectronic properties of semiconductors and is widely employed in the characterization of conventional III-V alloys, such as  $\text{GaAs}_{1-x}\text{P}_x$ ,<sup>1</sup>  $\text{Ga}_{1-x}\text{Al}_x\text{N}$ ,<sup>3</sup> and  $\text{GaAs}_{1-x}\text{N}_x$ .<sup>4</sup>

Considerable attention has recently been paid to wurtzite ZnO-based semiconductors, related heterostructures, and quantum wells<sup>5</sup> as a promising emerging material for light-emitting devices (LEDs), and ultraviolet photodetectors due to its superior physical properties of a direct wide bandgap (3.36 eV) and large excitonic binding energy (60 meV) at room temperature.<sup>6</sup> Besides the well-known *p*-type difficulty, one of the indispensable issues to be achieved is the bandgap engineering for the commercialization of ZnO-based optoelectronic devices. ZnMgO alloy system can provide an optically tunable family of wide bandgap materials in the range of  $\sim 3.3\text{--}7.5$  eV. Multiphonon scattering processes have been studied in detail for ZnO,<sup>7-9</sup> while there is significantly less work on the interesting topic of multiphonon RRS in ZnMgO,<sup>10</sup> although optical properties of ZnMgO have been extensively reported.<sup>11,12</sup> In this letter, we have presented an easy and effective way to comparatively investigate the RRS of longitudinal optical (LO) phonons in hexagonal  $\text{Zn}_{1-x}\text{Mg}_x\text{O}$  ( $x \leq 0.323$ ) thin films. The resonance effect is achieved by changing the Mg composition and sample temperature to tune the ZnMgO bandgap.

$\text{Zn}_{1-x}\text{Mg}_x\text{O}$  thin films were grown on *c*-plane sapphire (0001) substrates by pulsed laser deposition system employ-

ing a plasma oxygen source or gaseous oxygen source at the substrate temperature of 600 °C. The O plasma source was introduced by a plasma generator, with the working voltage of 400 V and the current of 35 mA. Ceramic ZnMgO targets were ablated by a KrF excimer laser (wavelength of 248 nm, energy of 200 mJ/pulse, and repetition rate of 5 Hz). The Mg compositions were characterized by a physics electronics instruments Quantum 2000 x-ray photoelectron spectroscopy. Microscopic RRS spectra were recorded in a backscattering geometry of  $z(x,-)\bar{z}$  configuration using a Jobin Yvon LabRAM HR 800UV micro-Raman system under a He-Cd laser (325 nm) at  $\sim 25$  mW power.

Figure 1(a) presents the room-temperature RRS spectra of five hexagonal  $\text{Zn}_{1-x}\text{Mg}_x\text{O}$  thin films with different Mg compositions. The sharp Raman peaks can be attributed to the LO phonon modes, and multiple scattering by the polar LO phonon is clearly observed up to the third order in ZnMgO alloys and fourth order in pure ZnO. At the measured temperature and laser power, we can only observe the free exciton transition in ZnO,<sup>13</sup> and the observed free exciton in ZnO transits to the localized exciton nature in ZnMgO alloy due to the Mg dopant in ZnO. We have therefore experienced the subtraction of only one kind of LO phonon regression

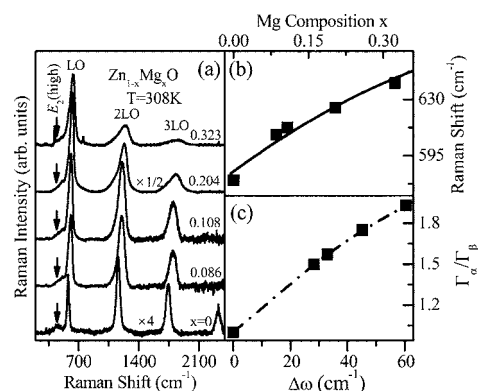


FIG. 1. (a) Room-temperature RRS spectra of ZnMgO thin films with different Mg compositions. (b) First-order LO phonon frequency (filled squares) in ZnMgO as a function of Mg composition  $x$ . The solid curve is the calculated result using the MREI model. (c) Different asymmetry  $\Gamma_a/\Gamma_b$  versus the first-order LO phonon Raman shift  $\Delta\omega$  with respect to that in pure ZnO. Dash-dotted curve is drawn as a guide to the eye.

a) Author to whom correspondence should be addressed. Electronic mail: wzshen@sjtu.edu.cn.

from the luminescence emission. Great enhancement of the LO phonons has been demonstrated as compared to the almost imperceptible modes of  $E_2$  (high) [marked as arrows in Fig. 1(a)].<sup>14</sup> The LO phonons shift to higher frequency and asymmetrically broaden as the Mg composition increases. These phonon behaviors are characteristics of resonant scattering in polar semiconductors,<sup>3</sup> which will provide much physical information on the alloy disorder effect and electronic state localization.<sup>10</sup>

The blueshift of the LO phonons in  $\text{Zn}_{1-x}\text{Mg}_x\text{O}$  alloys is mainly due to the fact that Zn–O bonds undergo a compressive strain because of the lattice mismatch between ZnO and MgO, which increases the effective force constant referred as compositional disorder of the alloy.<sup>1</sup> In Fig. 1(a), the dependence of LO phonons in  $\text{Zn}_{1-x}\text{Mg}_x\text{O}$  on the Mg composition exhibits one-mode vibration, as expected from the modified random element isodisplacement (MREI) model,<sup>11,12</sup> since the mass of substituting element Mg is larger than the reduced mass of ZnO. Figure 1(b) displays the first-order ZnO-like LO phonon frequency as a function of Mg composition, where the MREI model can well explain the experimental observation. On the other hand, in contrast to the symmetric Lorentzian profile of the Raman lineshape in the pure ZnO, the degree of asymmetry in the first-order LO phonon peaks of  $\text{Zn}_{1-x}\text{Mg}_x\text{O}$  increases with the Mg composition. Figure 1(c) shows the asymmetric ratio  $\Gamma_\alpha/\Gamma_\beta$  versus the frequency shift  $\Delta\omega$  with respect to that of pure ZnO, where  $\Gamma_\alpha$  ( $\Gamma_\beta$ ) is defined as the low- (high-) frequency half width at half maximum in the phonon line. The increasing potential fluctuation due to Mg incorporation causes lattice defect and structural disorder which basically results in the breakdown of the translational symmetry at wave vector  $q=0$ , and the contribution of Brillouin zone edges phonons to the Raman lineshape, i.e., greatly drives the lineshape asymmetry.

The observed asymmetric LO Raman lineshape suggests that the intermediate electronic state involved in resonant Raman process is strongly spatially localized.<sup>4</sup> Alloying compositional disorder brings localized electronic states in the forbidden bandgap of ZnMgO, which leads to a localized exciton-LO-phonon complex due to the strong coupling of the localized exciton to the most energetic LO phonon.<sup>1,3</sup> To better understand the localized electronic states in ZnMgO alloys introduced by the alloy disorder, we resort to Loudon's model for the band-to-band transition<sup>1</sup> and a simple atomistic model proposed by Balkanski *et al.*<sup>15</sup> for the excitonic localization. The Raman intensities of the first-, second-, and third-order LO phonon modes can be expressed respectively as

$$I(1\text{LO}) = A \left\{ \frac{z^2(1-z^2)^2}{[\hbar\omega_i - \hbar\omega(1\text{LO}) - \varepsilon_0]^2 + \gamma^2} \right\}, \quad (1)$$

$$I(2\text{LO}) = \frac{A}{2} \left\{ \frac{z^4(1-2z^2+z^4/2)^2}{[\hbar\omega_i - \hbar\omega(2\text{LO}) - \varepsilon_0]^2 + \gamma^2} \right\}, \quad (2)$$

$$I(3\text{LO}) = \frac{A}{6} \left\{ \frac{z^6(1-3z^2+3z^4/2-z^6/6)^2}{[\hbar\omega_i - \hbar\omega(3\text{LO}) - \varepsilon_0]^2 + \gamma^2} \right\}, \quad (3)$$

where  $A$  is related to the band-to-band transition,<sup>1</sup>  $z$  is ratio of the coupling constant of the localized exciton to the LO phonon energy,  $\varepsilon_0$  is the bandgap energy,  $\gamma$  is the width of the localized exciton,  $\hbar\omega_i$  is the incident photon energy, and  $\hbar\omega(1\text{LO})$ ,  $\hbar\omega(2\text{LO})$ , and  $\hbar\omega(3\text{LO})$  are the first-, second-, and third-order LO phonon energies, respectively.

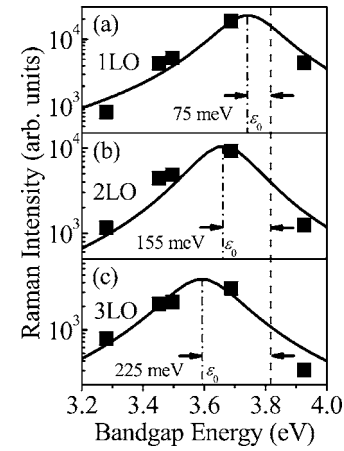


FIG. 2. Resonance behavior of the (a) first-order LO, (b) second-order LO, and (c) third-order LO phonons at room temperature. The filled squares are experimental data and solid curves are the theoretical calculation via Eqs. (1)–(3). The dashed line is the energy of the 325 nm laser.

and third-order phonon energies, respectively.

The resonance enhancement of LO phonons can be achieved by different Mg composition tuning of the ZnMgO bandgap. The effect of tuning Mg composition is equivalent to changing the photon energy of the laser by an amount equal in magnitude and opposite in sign to the corresponding change in bandgap. Figure 2 presents the Raman intensity of the first-, second-, and third-order LO phonon modes in Fig. 1(a) as a function of ZnMgO bandgap energies  $E_g$  at room temperature, which have been obtained from the transmission measurements. A good agreement between the theoretical results and experimental data has been demonstrated for all the three LO modes with the same  $z$  of 2.5 and  $\gamma$  of 113 meV. The larger coupling constant ratio  $z$  in ZnMgO in comparison with the III-V semiconductors ( $\sim 0.9$ ) (Ref. 1) accounts for the occurrence of the higher-order multiphonon resonances, since the intensity of multiphonon Raman scattering is roughly proportional to the square of the polaron coupling and consequently correlated with the polarity of the anion-cation bond.<sup>16</sup> During the fitting, the relative contributions of the excitonic localization and the band-to-band transition to RRS ( $z/A$ ) is found to be 1.68, 20.83, and 13.68 for the first-, second-, and third-order LO phonons, respectively. It is clear that the localized exciton dominates the LO phonon resonances, especially in the higher-order (second- and third-order) LO phonon resonances. This can be explained in terms of the fact that the excitonic binding energy in ZnMgO is closed to the LO-phonon energy ( $\sim 75$  meV), and hence, increases the available phase space for the exciton-LO-phonon scattering process.<sup>10</sup>

Furthermore, we note that the maximum of the Raman intensity takes place 75 meV (in the first order), 155 meV (second order), and 225 meV (third order) lower away from the incident photon energy of the laser. These values correspond well to the energies of one, two, and three LO phonons, indicating that these three Raman processes are outgoing first-, second-, and third-order LO phonon resonances. The involvement of the localized exciton reveals that the main mechanism of the outgoing resonance is due to the extrinsic Fröhlich interaction mediated via a localized exciton. In addition, it is well known that the excitonic linewidth is usually related to the lifetime of excitons, and we can simply estimate the lifetime of localized exciton by  $\tau$

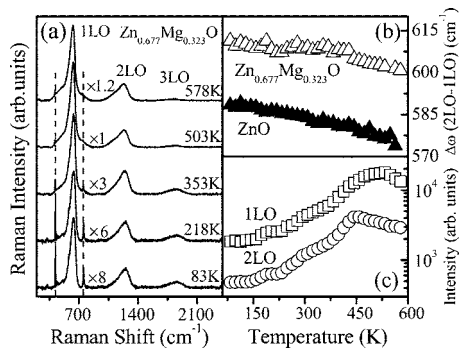


FIG. 3. Temperature-dependent (a) RRS spectra of  $\text{Zn}_{0.677}\text{Mg}_{0.323}\text{O}$  with the sapphire phonon modes marked by the vertical dashed lines, (b) frequency difference between the second- and first-order LO phonons in  $\text{Zn}_{0.677}\text{Mg}_{0.323}\text{O}$  (open triangles) and  $\text{ZnO}$  (filled triangles), and (c) intensity of the first-order (open squares) and second-order (open circles) LO phonons in  $\text{Zn}_{0.677}\text{Mg}_{0.323}\text{O}$ .

$=h/\pi\gamma$ .<sup>1</sup> This gives  $\tau=1.17$  fs at room temperature for the localized exciton. The shorter lifetime of the localized exciton suggests a positive effect on the high optical efficiency of  $\text{ZnO}$ -based LEDs.<sup>17</sup>

To support the argument that localized excitonic contribution for the second-order LO phonon is larger than that for the first-order one, we can further examine the resonance effect by temperature tuning of the material bandgap.<sup>1</sup> The effect of changing the temperature is similar to that of tuning Mg composition in  $\text{ZnMgO}$  of Fig. 1(a). Figure 3(a) shows that the energy of the fundamental bandgap is tuned into resonance with the incident photon energy by varying the sample temperature from 83 to 578 K for the  $\text{Zn}_{1-x}\text{Mg}_x\text{O}$  ( $x=0.323$ ) alloy. Resonantly enhanced first- and second-order LO phonon modes are clearly observed. The LO phonon modes shift to lower frequency and broaden with the increase of sample temperature, which may be attributed to the contribution of the thermal expansion of lattice and anharmonic decay of phonons into two and three phonons.<sup>18</sup> The first- and second-order LO phonon modes become dominant with increasing temperature from 83 to  $\sim 430$ –530 K, for which the fundamental bandgap energy  $E_g$  of  $\text{Zn}_{0.677}\text{Mg}_{0.323}\text{O}$  decreases and brings into resonance with the incident photon energy. Further increase of the temperature the LO phonon mode intensity decreases as the bandgap energy  $E_g$  is reduced to be lower than the incident photon energy.

Figure 3(b) displays the temperature-dependent frequency difference  $\Delta\omega(2\text{LO}-1\text{LO})$  between the second- and first-order LO phonons in both  $\text{ZnO}$  and  $\text{Zn}_{0.677}\text{Mg}_{0.323}\text{O}$ . We note that  $\text{ZnO}$  exhibits the faster approximated linear downshift (with a slope of  $\sim 2.78 \times 10^{-2} \text{ cm}^{-1}/\text{K}$ ) than that of  $\text{Zn}_{0.677}\text{Mg}_{0.323}\text{O}$  ( $\sim 1.63 \times 10^{-2} \text{ cm}^{-1}/\text{K}$ ). As we know, the localized excitonic effect compensates the frequency downshift of the first- and second-order LO phonons in  $\text{ZnMgO}$  with the increasing temperature.<sup>19</sup> If the compensation effect is the same for both the first- and second-order LO phonons in  $\text{ZnMgO}$ , we would expect the same temperature-dependent behavior of  $\Delta\omega(2\text{LO}-1\text{LO})$  in  $\text{Zn}_{0.677}\text{Mg}_{0.323}\text{O}$  and  $\text{ZnO}$ . The observed slow frequency downshift in  $\text{ZnMgO}$  can be explained only when the localized excitonic compensating effect is larger in the second-order LO phonon than that in the first-order one. Therefore, we can conclude from the compensation of frequency downshift that the localized excitonic contribution in the second-order LO phonon is

larger than that of the first-order one in RRS, which is in good agreement with the observation in Fig. 2. In addition, we also observe the fast downshift in the frequency above  $\sim 450$  K in  $\text{Zn}_{0.677}\text{Mg}_{0.323}\text{O}$ , which can be attributed that excitons undergo transitions from localized to delocalized states due to thermal energy increasing with temperature.

Finally, we present the further evidence for the outgoing Raman resonance. Figure 3(c) illustrates the first- and second-order phonon intensity of  $\text{Zn}_{0.677}\text{Mg}_{0.323}\text{O}$  versus temperature. The maxima for the first- and second-order LO phonon intensity are exhibited at  $\sim 530$  and  $\sim 430$  K, respectively. Based on the assumption that the temperature-dependent bandgap energy of  $\text{Zn}_{0.677}\text{Mg}_{0.323}\text{O}$  is the same as that of  $\text{ZnO}$  reported in Ref. 20, we can deduce that the energy separation between the first- and second-order LO phonon intensity maxima is  $\sim 70$  meV, which is closed to the LO phonon energy of 75 meV. Similar to the observation in Figs. 2(a) and 2(b), this behavior is also indicative of an outgoing resonance nature in RRS. The small energy difference may be due to the fact that for the second-order RRS, the phonons are no longer restricted to the center of the Brillouin zone and the alloy-induced disorder brings up an increase of phonon density of states. As a consequence, the difference energy between the second- and first-order LO phonon bands will be a slightly lower than the LO phonon energy.

This work was supported by the Natural Science Foundation of China under Contract No. 10734020, and the National Minister of Education Program of IRT0524.

- <sup>1</sup>C. Ramkumar, K. P. Jain, and S. C. Abbi, *Phys. Rev. B* **54**, 7921 (1996).
- <sup>2</sup>J. Ding, H. Jeon, T. Ishihara, M. Hagerott, A. V. Nurmikko, H. Luo, N. Samarth, and J. Furdyna, *Phys. Rev. Lett.* **69**, 1707 (1992).
- <sup>3</sup>F. Demangeot, J. Frandon, M. A. Renucci, H. S. Sands, D. N. Batchelder, O. Briot, and S. Ruffenach-Clur, *Solid State Commun.* **109**, 519 (1999).
- <sup>4</sup>A. Mascarenhas, M. J. Seong, S. Yoon, J. C. Verley, J. F. Geisz, and M. C. Hanna, *Phys. Rev. B* **68**, 233201 (2003).
- <sup>5</sup>A. Tsukazaki, A. Ohtomo, T. Kita, Y. Ohno, and M. Kawasaki, *Science* **315**, 1388 (2007).
- <sup>6</sup>M. H. Huang, S. Mao, H. Feick, H. Q. Yan, Y. Y. Wu, H. Kind, E. Weber, R. Russo, and P. D. Yang, *Science* **292**, 1897 (2001).
- <sup>7</sup>V. V. Ursaki, I. M. Tiginyanu, V. V. Zalamai, E. V. Rusu, G. A. Emelchenko, V. M. Masalov, and E. N. Samarov, *Phys. Rev. B* **70**, 155204 (2004).
- <sup>8</sup>X. T. Zhang, Y. C. Liu, Z. Z. Zhi, J. Y. Zhang, Y. M. Lu, D. Z. Shen, W. Xu, G. Z. Zhong, X. W. Fan, and X. G. Kong, *J. Phys. D* **34**, 3430 (2001).
- <sup>9</sup>H. M. Cheng, K. F. Lin, H. C. Hsu, and W. F. Hsieh, *Appl. Phys. Lett.* **88**, 261909 (2003).
- <sup>10</sup>J. D. Ye, K. W. Teoh, X. W. Sun, G. Q. Lo, D. L. Kwong, H. Zhao, S. L. Gu, R. Zhang, Y. D. Zheng, S. A. Oh, X. H. Zhang, and S. Tripathy, *Appl. Phys. Lett.* **91**, 091901 (2007).
- <sup>11</sup>J. Chen and W. Z. Shen, *Appl. Phys. Lett.* **83**, 2154 (2003).
- <sup>12</sup>C. Bundesmann, A. Rahm, M. Lorenz, M. Grundmann, and M. Schubert, *J. Appl. Phys.* **99**, 113504 (2006).
- <sup>13</sup>H. Najafov, Y. Fukada, S. Ohshio, S. Iida, and H. Saitoh, *Jpn. J. Appl. Phys., Part 1* **42**, 3490 (2003).
- <sup>14</sup>K. A. Alim, V. A. Fonoberov, and A. A. Balandin, *Appl. Phys. Lett.* **86**, 053103 (2005).
- <sup>15</sup>M. Balkanski, L. M. Falikov, C. Hirlimann, and K. P. Jain, *Solid State Commun.* **25**, 261 (1978).
- <sup>16</sup>K. Miwa and A. Fukumoto, *Phys. Rev. B* **48**, 7897 (1993).
- <sup>17</sup>S. Chichibu, T. Azuhata, T. Sota, and S. Nakamura, *Appl. Phys. Lett.* **69**, 4188 (1996).
- <sup>18</sup>L. L. Guo, Y. H. Zhang, and W. Z. Shen, *Appl. Phys. Lett.* **89**, 161920 (2006).
- <sup>19</sup>D. Behr, J. Wagner, A. Ramakrishnan, H. Obloh, and K. H. Bachem, *Appl. Phys. Lett.* **73**, 241 (1998).
- <sup>20</sup>H. B. Ye, J. F. Kong, W. Z. Shen, J. L. Zhao, and X. M. Li, *J. Phys. D* **40**, 5588 (2007).